Author Manuscript

Author Manuscript

Author Manuscript

Author Manuscript

HHS Public Access

Author manuscript

Neurobiol Aging. Author manuscript; available in PMC 2020 May 01.

Published in final edited form as:

Neurobiol Aging. 2019 May ; 77: 104–111. doi:10.1016/j.neurobiolaging.2019.01.022.

Associations of Amygdala Volume and Shape with Transactive Response DNA-binding Protein 43 (TDP-43) Pathology in a Community Cohort of Older Adults

Nazanin Makkinejad[a], **Julie A. Schneider**[b,c,d], **Junxiao Yu**[a], **Sue E. Leurgans**[b,d], **Aikaterini Kotrotsou**[a], **Arnold M. Evia**[a], **David A. Bennett**[b,d], and **Konstantinos Arfanakis**[a,b,e]

[a]Department of Biomedical Engineering, Illinois Institute of Technology, Chicago, Illinois, USA.

[b]Rush Alzheimer's Disease Center, Rush University Medical Center, Chicago, Illinois, USA.

[c]Department of Pathology, Rush University Medical Center, Chicago, Illinois, USA.

[d]Department of Neurological Sciences, Rush University Medical Center, Chicago, Illinois, USA.

[e]Department of Diagnostic Radiology, Rush University Medical Center, Chicago, Illinois, USA.

Abstract

Transactive response DNA-binding protein 43 (TDP-43) pathology is common in old age and is strongly associated with cognitive decline and dementia above and beyond contributions from other neuropathologies. TDP-43 pathology in aging typically originates in the amygdala, a brain region also affected by other age-related neuropathologies such as Alzheimer's pathology. The purpose of this study was two-fold: to determine the independent effects of TDP-43 pathology on the volume, as well as shape, of the amygdala in a community cohort of older adults, and to determine the contribution of amygdala volume to the variance of the rate of cognitive decline after accounting for the contributions of neuropathologies and demographics. Cerebral hemispheres from 198 participants of the Rush Memory and Aging Project and the Religious Orders Study were imaged with MRI ex-vivo and underwent neuropathologic examination. Measures of amygdala volume and shape were extracted for all participants. Regression models controlling for neuropathologies and demographics showed an independent negative association of TDP-43 with the volume of the amygdala. Shape analysis revealed a unique pattern of amygdala deformation associated with TDP-43 pathology. Finally, mixed effects models showed that amygdala volume explained an additional portion of the variance of the rate of decline in global cognition, episodic memory, semantic memory, and perceptual speed, above and beyond what was explained by demographics and neuropathologies.

Correspondence to: Konstantinos Arfanakis, PhD, 3440 South Dearborn St., M-102, Chicago, IL, 60616, Phone: (312) 567-3864, arfanakis@iit.edu.

Disclosure Statement

The authors have no financial interests or relationships to disclose with regard to the subject matter of this manuscript.

Publisher's Disclaimer: This is a PDF file of an unedited manuscript that has been accepted for publication. As a service to our customers we are providing this early version of the manuscript. The manuscript will undergo copyediting, typesetting, and review of the resulting proof before it is published in its final citable form. Please note that during the production process errors may be discovered which could affect the content, and all legal disclaimers that apply to the journal pertain.

Author Manuscript Author Manuscript Author Manuscript Author Manuscript

Keywords

MRI; ex-vivo; pathology; amygdala; TDP-43; Alzheimer's; hippocampal sclerosis; volume; shape; cognitive decline

1. Introduction

Transactive response DNA-binding protein 43 (TDP-43) pathology, the primary protein abnormality in the rare, typically presenile, neurodegenerative diseases frontotemporal lobar degeneration and amyotrophic lateral sclerosis (Neumann et al., 2006), is now recognized as a common age-related neuropathology, detected at autopsy in approximately 50% of older persons. TDP-43 pathology has been reported in up to 55% of persons with Alzheimer's disease (AD) pathology (Arai et al., 2009; Tremblay et al., 2011), 60% of persons with Lewy bodies (Arai et al., 2009), 90% of persons with hippocampal sclerosis (Zarow et al., 2012), and in other neurodegenerative diseases (Freeman et al., 2008; Fujishiro et al., 2009; Geser et al., 2008; Lippa et al., 2010; Olivé et al., 2009; Schwab et al., 2009, 2008; Uryu et al., 2013; Wider et al., 2009). Yet, TDP-43 has also been detected in normal older persons (Arnold et al., 2013; Davidson et al., 2011; Geser et al., 2010; Mcaleese et al., 2016; Uchino et al., 2015; Wilson et al., 2013). The effect of TDP-43 pathology on cognition of older adults is devastating. TDP-43 pathology in aging is strongly and independently associated with cognitive decline and increased risk of dementia above and beyond the contributions of other age-related neuropathologies (Josephs, 2010; Nelson et al., 2010; Wilson et al., 2013). Moreover, TDP-43 pathology in aging has been shown to account for nearly as much of the variance of late-life cognitive decline as neurofibrillary tangles (hallmark pathology of AD) (Wilson et al., 2013). Thus, TDP-43 pathology is now recognized as a common and deleterious neuropathology of the aging brain.

Deposition of TDP-43 pathology in aging typically begins, and is most commonly seen, in the amygdala. In persons with Alzheimer's disease, it was previously shown that TDP-43 pathology is first deposited in the amygdala, followed by the hippocampus and entorhinal cortex, and then the neocortex and other regions (James et al., 2016; Josephs et al., 2014a). In cases with Lewy bodies with no or low tau burden, the amygdala was shown to have TDP-43 inclusions in all TDP-43 positive cases, while other regions were less frequently affected by TDP-43 (e.g. the entorhinal cortex, followed by the hippocampus and other cortical regions) (Yokota et al., 2010). In progressive supranuclear palsy, TDP-43 was again found most frequently in the amygdala, followed by hippocampus, entorhinal cortex, and other regions (Koga et al., 2016). In persons with hippocampal sclerosis, TDP-43 inclusions were most frequent in the amygdala compared to other brain regions (Nag et al., 2015). In older adults who were cognitively normal at the time of death, the amygdala was again the most common location for TDP-43 deposition (Arnold et al., 2013). In community-dwelling older adults, the amygdala exhibited TDP-43 inclusions in all individuals with the pathology, and as TDP-43 progressed from the amygdala to the hippocampus or entorhinal cortex and to the neocortex, there was a gradual increase of inclusions in the amygdala (Nag et al., 2018). The above findings suggest that the amygdala is involved early on in the progression of TDP-43 in aging, and is most often affected by TDP-43 pathology compared to any other

Author Manuscript Author Manuscript Author Manuscript Author Manuscript

brain region. Therefore, identifying amygdala abnormalities that are linked to TDP-43 pathology in aging and are detectable by MRI may be of high significance for the development of future strategies for the detection of the pathology.

Little is known about MR-detectable amygdala abnormalities associated with TDP-43 pathology in aging. A single recent MR-volumetry and pathology study on 248 older adults with pathologic diagnosis of AD and 46 controls showed a significant association between lower amygdala volumes and TDP-43 pathology (Josephs et al., 2014b). However, MRI was conducted in-vivo, allowing additional pathology to develop between imaging and autopsy, thereby potentially underestimating the effects of pathology on brain MR characteristics. Furthermore, all MRI scans were conducted between 1992–2010, primarily on 1.5 Tesla (T) scanners, suggesting potentially high coefficient of variation for volume measurements in small brain regions such as the amygdala, especially for data collected on older scanners. In addition, although analyses controlled for an extensive list of neurodegenerative pathologies, infarcts were the only vascular pathology controlled for. To our knowledge, there are no reports in the literature on amygdala shape abnormalities associated with TDP-43 pathology in aging. Shape analysis can provide important information on the spatial distribution of atrophy or expansion of a structure that exhibits volume abnormalities, and based on the substructures involved and their functional role may aid in understanding the functional outcomes of such volume abnormalities. Finally, no studies on the links between amygdala structural abnormalities and TDP-43 pathology in aging have been conducted in a community cohort.

The purpose of this study was to determine the independent effects of TDP-43 pathology in aging on both the volume and shape of the amygdala, by combining ex-vivo MRI and pathology in a large community cohort of older adults. By using ex-vivo MRI, no additional pathology developed between imaging and pathologic examination, and frail older adults were not excluded from MRI, thereby eliminating two important biases. Clinical 3T MRI scanners and pulse sequences were used in order to generate sufficient data quality while enhancing in-vivo translation of potential findings. A comprehensive set of age-related neuropathologies was considered in analyses to more accurately delineate the independent effects of TDP-43 pathology in aging. Shape analysis was used in addition to volumetry to extract the unique amygdala deformation pattern associated with TDP-43, which may be more informative than global amygdala volume changes alone. Finally, the contribution of amygdala volume to the variance of the rate of cognitive decline was assessed, after accounting for the contributions of neuropathologies and demographics. This study was conducted in a community cohort to enhance the generalizability of potential findings.

2. Methods

2.1 Study population

Individuals enrolled in two longitudinal clinical-pathologic cohort studies of aging, the Rush University Memory and Aging Project (MAP) and the Religious Order Study (ROS) (Bennett et al., 2018), were included in this investigation. Both studies were approved by the institutional review board of Rush University Medical Center. All participants provided written informed consent and signed an anatomical gift act. Annual clinical evaluation

Author Manuscript Author Manuscript Author Manuscript Author Manuscript

including cognitive function testing, medical history, and neurologic examination was performed on all participants. Diagnosis of dementia and Alzheimer's disease was based on the criteria of the National Institute of Neurological and Communicative Disorders and Stroke and the Alzheimer Disease and Related Disorders Association (NINCDS/ADRA) (McKhann et al., 1984). Participants who had cognitive impairment but did not meet the criteria for dementia were classified as having mild cognitive impairment (MCI) (Bennett et al., 2002; Boyle et al., 2006). At the time of these analyses, 3194 MAP/ROS participants had completed the baseline clinical evaluation. Of these, 572 died and 78 withdrew from the study before the ex-vivo MRI sub-study began. Of the remaining 2544 persons, 952 died, 816 were autopsied, and 646 had ex-vivo MRI. Amygdala segmentation was conducted in the first 208 consecutive cases. Of these 208 persons, 2 did not have TDP-43 pathology data, and 8 failed the subsequent shape analysis procedure. Hence, analyses were performed on the first 198 eligible participants (Table 1).

2.2 Cognitive testing

A battery of 21 cognitive tests was administered to all participants annually. One of the tests, the Mini-Mental State Examination, was used only for descriptive purposes, and a second test, the Complex Ideational Material, was used only for diagnostic purposes. The remaining 19 tests were used to evaluate performance in five cognitive domains: 7 tests for episodic memory, 3 for semantic memory, 3 for working memory, 4 for perceptual speed, and 2 for visuospatial ability (Bennett et al., 2018). Raw scores for each test were converted to z-scores, and were averaged across all 19 tests to obtain a composite score of global cognition (Wilson et al., 2003). For each cognitive domain, the z-scores from the corresponding tests were also averaged into a composite score for that cognitive domain (Bennett et al., 2006).

2.3 Brain hemisphere preparation

Upon a participant's death, an autopsy technician removed the brain, and the cerebrum was separated from the cerebellum and brainstem. The cerebrum was divided into the left and right hemispheres by cutting the corpus callosum, and the hemisphere with more visible pathology was selected for ex-vivo MRI and pathologic examination, while the contralateral hemisphere was frozen and stored. The selected hemisphere was immersed in phosphate-buffered 4% formaldehyde solution and refrigerated at 4°C, within 30 minutes of removal from the skull. Ex-vivo MRI was conducted while the hemisphere was immersed in formaldehyde solution with its medial aspect facing the bottom of an MR-compatible container, at room temperature. Gross examination was performed within 2 weeks after ex-vivo MRI, followed by histopathologic diagnostic examination by a board-certified neuropathologist (Kotrotsou et al., 2015).

2.4 Ex-vivo MRI data acquisition and pre-processing

All imaging data were collected on 3 Tesla MRI scanners (Table 1) using a 2D spin-echo sequence with multiple echo times. Due to the ongoing nature of this study and scanner upgrades, three MRI scanners with similar imaging protocols were used for data collection (Dawe et al., 2014). The voxel size was $0.6 \times 0.6 \times 1.5\ mm^3$ for all scanners, and only T2-weighted images collected at echo times between 50–58 ms were used in the analysis.

Author Manuscript Author Manuscript Author Manuscript Author Manuscript

The gray matter of the T2-weighted image volumes from all hemispheres was segmented into 42 cortical and subcortical regions using a published multi-atlas approach based on 25 atlases (Kotrotsou et al., 2014), and amygdala segmentation in each hemisphere was further refined using manual corrections (Fig.1). The volume of the amygdala was calculated for each hemisphere as the product of the number of voxels within the segmented region and the voxel volume. The amygdala volume was then normalized by the participant's height, which has previously been used as a surrogate for total intracranial volume (Dawe et al., 2011; Kotrotsou et al., 2015; Van Petten, 2004).

Since surface alignment is not well-defined on shapes with rotational symmetry such as the amygdala (Styner et al., 2003), initial correspondence of amygdala surfaces was established by whole hemisphere registration. More specifically, the image volumes from all hemispheres were rigidly registered to a template using FSL (FMRIB, Oxford, UK) (Smith et al., 2004). The resulting rigid body transforms were then applied to the amygdala masks.

2.5 Shape analysis

Shape analysis was conducted using the spherical harmonic basis function toolbox SPHARM-PDM (Styner et al., 2006). For each hemisphere, the rigidly transformed amygdala mask from the previous step was smoothed using level set based anti-alias smoothing. A triangulated mesh was generated on the surface of the amygdala mask, and a spherical parameterization was obtained by mapping the mesh to a sphere using an area preserving and distortion minimizing spherical mapping algorithm. SPHARM represents an original surface through a weighted linear combination of spherical harmonic basis functions. The spherical harmonic degree was set at 15. The parameterization was then sampled with icosahedron subdivision at level 10, which formed a triangulated mesh with 1002 vertices on the amygdala surface. The meshes from all hemispheres were spatially aligned using the Procrustes rigid body transformation, were normalized with the participants' height, and were averaged. For each hemisphere, the difference vector from a vertex on the average mesh to the corresponding vertex on the individual hemisphere's mesh was calculated, and the process was repeated for all vertices. Each difference vector was then projected to the normal vector on the corresponding vertex of the average mesh to obtain a signed shape difference of an individual's amygdala from the average. The signed shape differences were used in statistical analysis (see below).

2.6 Neuropathologic evaluation

Following MRI, each hemisphere was sectioned into 1-cm thick coronal slabs. The slabs underwent macroscopic evaluation and dissection of selected tissue blocks, which were embedded in paraffin, cut into sections, and mounted on glass slides. Neuropathologic evaluation was completed by a board-certified neuropathologist blinded to all clinical data and age, and following well-established procedures. A detailed description of neuropathologic evaluation can be found in Kotrotsou et al., 2015. The score assigned to each neuropathology represented the global burden in the hemisphere and not specifically in the amygdala. TDP-43 was rated on four levels capturing the staging of the pathology (no inclusions; inclusions in amygdala only; inclusions in amygdala as well as entorhinal cortex or hippocampus CA1; and inclusions in amygdala, entorhinal cortex or hippocampus CA1,

Author Manuscript Author Manuscript Author Manuscript Author Manuscript

and neocortex) (Yu et al., 2015). A composite score of global AD pathology was given for each hemisphere based on plaque and tangle counts in 5 brain regions (Schneider et al., 2007). Hippocampal sclerosis was rated as present or absent (Schneider et al., 2009). Lewy bodies were detected in 6 regions and were rated as present or absent (McKeith et al., 1996; Schneider et al., 2012). Gross infarcts were scored as none, one, or more than one. Microscopic infarcts were detected in a minimum of 9 regions and were scored as none, one, or more than one (Arvanitakis et al., 2011a). Atherosclerosis and arteriolosclerosis were scored as none, mild, moderate, and severe. Cerebral amyloid angiopathy was assessed in 4 regions and was rated as none, mild, moderate, and severe (Arvanitakis et al., 2011b).

2.7 Statistical analysis

The least absolute shrinkage and selection operator (LASSO) approach was employed to investigate the association of amygdala volume (dependent variable), as well as signed shape differences at all vertices of the average mesh (dependent variables), with (independent variables) TDP-43, hippocampal sclerosis, AD pathology, Lewy bodies, arteriolosclerosis, atherosclerosis, gross and microscopic infarcts, and cerebral amyloid angiopathy, while controlling for age at death, sex, years of education, scanner, duration between death and immersion in formaldehyde solution (post mortem interval to fixation, PMI), and duration between death and ex-vivo MRI (post mortem interval to imaging, PMII). LASSO is a penalized regression model, where an l_1 regularization is added to the standard multiple linear regression model. The optimal penalty factor was calculated by a leave-one-out cross validation procedure by minimizing the mean squared error and enforcing sparsity in the output model. All models were implemented in R version 3.4.0 (The R Foundation for Statistical Computing). For the signed shape differences, p-values were corrected for multiple comparisons using the false discovery rate (FDR) approach (Benjamini and Hochberg, 1995). Associations of amygdala volume and signed shape differences with neuropathologies were considered significant at $p<0.05$. The Shape Population Viewer Toolbox (www.nitrc.org/projects/shapepopviewer/) was used for visualization of shape analysis results.

Two linear mixed-effects models were used to assess the contribution of amygdala volume measured ex-vivo to the variance of the rate of decline in global cognition above and beyond what was explained by neuropathologies and demographics. The composite score of global cognition was the longitudinal dependent variable in both models. The independent variables in the first model were all the neuropathologies, demographics and covariates listed in the previous paragraph, as well as the interaction of each one of these variables with time since baseline. The independent variables in the second model included those of the first model plus the volume of the amygdala and its interaction with time since baseline. The percent difference in the variance of the rate of decline between the two mixed-effects models provided the additional percentage of variance explained by amygdala volume above and beyond what was explained by pathologies and demographics. Both models were implemented in R version 3.4.0 (The R Foundation for Statistical Computing), and the additional variance explained by amygdala volume was considered significant when the interaction term of amygdala volume with time since baseline was statistically significant ($p<0.05$). The same analysis was repeated for each of the five cognitive domains.

Author Manuscript Author Manuscript Author Manuscript Author Manuscript

Results

3.1 Demographic, clinical and neuropathologic characteristics

Demographic and clinical characteristics of the participants are presented in Table 1, and neuropathologic characteristics are presented in Table 2. When comparing this sample to 464 other participants of the parent studies who had an autopsy after the start of the present work, the present sample had on average 1.2 more years of education ($p<0.0001$), 0.2 lower global cognition score proximate to death ($p=0.048$), 0.22 lower working memory score ($p=0.02$), 0.38 lower visuospatial abilities score ($p<0.0001$), and more severe atherosclerosis (the 464 individuals were distributed as follows: none=26%, mild=52%, moderate=18%, severe=5%; compare to the atherosclerosis distribution shown in Table 2) ($p<0.0001$). No significant differences in amygdala volume were observed across scanners used in this work (ANOVA, $F(2,195) = 1.16$, $p=0.32$).

3.2 Associations of amygdala volume and shape with neuropathology

LASSO regression analysis showed a negative correlation of normalized amygdala volume with TDP-43 (model estimate=-31.5 mm^2, $p=0.0003$), AD pathology (model estimate=-75.0 mm^2, $p<10^{-4}$), and hippocampal sclerosis (model estimate=-95.4 mm^2, $p=0.0004$), but not with any other neuropathologies. The independent contributions of TDP-43, AD pathology, and hippocampal sclerosis on the surface of the amygdala are shown before and after FDR correction for multiple comparisons in Figures 2A and 2B, respectively. All parts of the amygdala surface with significant associations with neuropathologies showed inward deformation, and are represented with warm colors in Figure 2. Inward deformations associated with TDP-43 were located in portions of the centromedial, superficial, and laterobasal subdivisions of the amygdala (Fig.2B) (Amunts et al., 2005). Deformations linked to AD and hippocampal sclerosis were mainly in the superficial, and laterobasal subdivisions and were generally more extensive than those linked to TDP-43 (Fig.2B). Repeating all analyses after removing 2 of the 24 participants with hippocampal sclerosis that were TDP-43 negative, resulted in very similar associations of amygdala volume and shape with neuropathologies as those described above. Also, repeating all analyses in the group of 137 participants with intermediate or high likelihood of AD (according to NIA-Reagan criteria) resulted in very similar associations of amygdala volume and shape with neuropathologies as those described above. In contrast, repeating all analyses in the group of 61 participants with low likelihood or no AD did not result in any significant findings, which may be due to the small size of that group.

3.3 Contribution of amygdala volume to the variance of the rate of cognitive decline

Mixed-effects models revealed that, first, lower amygdala volume was independently associated with faster decline in global cognition (model estimate=$1.8\cdot10^{-4}$, $p=0.009$), episodic memory (model estimate=$1.7\cdot10^{-4}$, $p=0.027$), semantic memory (model estimate=$2.4\cdot10^{-4}$, $p=0.0012$), and perceptual speed (model estimate=$1.8\cdot10^{-4}$, $p=0.029$), controlling for neuropathologies, demographics and covariates (Table 3). Second, mixed-effects models also revealed that the amygdala volume explained an additional 8.1% of the variance of the rate of decline in global cognition, 5.3% of the variance of the rate of decline

Author Manuscript Author Manuscript Author Manuscript Author Manuscript

in episodic memory, 8.7% in semantic memory, and 3.8% in perceptual speed, above and beyond what was explained by neuropathologies and demographics (Table 3).

Discussion

The present study investigated the association of TDP-43 pathology in aging with the volume and shape of the amygdala by combining ex-vivo MRI and pathology on a community cohort of older adults. TDP-43 pathology in aging was found to be negatively correlated with the volume of the amygdala, independent of the effects of other neuropathologies. TDP-43 pathology in aging was also associated with a unique spatial pattern of inward deformation of the amygdala surface that was different than the patterns linked to AD pathology and hippocampal sclerosis. Finally, the volume of the amygdala was found to explain an additional portion of the variance of the rate of decline in global cognition, episodic memory, semantic memory, and perceptual speed, above and beyond what was explained by neuropathologies and demographics.

The finding showing an independent negative association of amygdala volume with TDP-43 pathology in aging is in general agreement with a recent report in persons with a pathologic diagnosis of AD (Josephs et al., 2014b). The present study extended the previous work to a community cohort with a range of cognitive function, enhancing generalization of the findings. In addition, the present study combined neuropathology and ex-vivo MRI, instead of in-vivo MRI, eliminating the possibility of additional pathology developing between imaging and autopsy, and thereby avoiding underestimation of the effects of pathology detected by MRI. Furthermore, use of ex-vivo, instead of in-vivo MRI ensured that participation in the present study was independent of frailty level. Additionally, a more comprehensive set of neurodegenerative and vascular neuropathologies, as well as demographics (Tang et al., 2017), was controlled for in the analyses of the present study. Thus, the current methodology extended previous work and more accurately delineated the independent effects of TDP-43 pathology on the volume of the amygdala in community-dwelling older adults.

Undoubtedly, investigating the volume of the amygdala alone cannot reveal the subtle differences between the effects of TDP-43 and other neuropathologies on amygdala structure. Shape analysis addressed this limitation and mapped the independent spatial pattern of amygdala deformation associated with TDP-43 pathology. Although the spatial extent of the TDP-43-related inward deformation of the amygdala surface was spatially more limited compared to that linked to AD pathology and hippocampal sclerosis, the shape abnormalities associated with TDP-43 involved the centromedial, superficial, and laterobasal subdivisions of the amygdala, while those associated with AD pathology and hippocampal sclerosis involved mainly the superficial and laterobasal subdivisions (Amunts et al., 2005). To our knowledge this is the first study mapping the independent spatial patterns of amygdala deformation associated with TDP-43 pathology and hippocampal sclerosis. Our finding that AD pathology is associated with superficial and laterobasal inward deformation with relative sparing of the centromedial subdivision is in general agreement with previous in-vivo MRI work on the association of clinical AD diagnosis with the shape of the amygdala (Miller et al., 2015; Qiu et al., 2009; Tang et al., 2015, 2014). This agreement

Author Manuscript Author Manuscript Author Manuscript Author Manuscript

serves as confirmation that ex-vivo MRI can provide similar information on amygdala shape as that originating from in-vivo MRI, increasing confidence on the novel TDP-43 and hippocampal sclerosis patterns generated here. In addition, our spatial pattern of AD-related amygdala deformation is in general agreement with neuropathologic reports on the distribution of neurofibrillary tangles and neuritic plaques in the amygdala (Kromer Vogt et al., 1990). On the other hand, a study by Cavedo et al., 2011, on 19 AD patients and 19 healthy controls, showed AD-related inward deformation even in the centromedial subdivision, while in the present work, centromedial deformation was only associated with TDP-43. Since, TDP-43 pathology is often present in persons with AD, and since the study by Cavedo et al., 2011, was based on clinical diagnosis of AD, the centromedial deformation seen in that previous study may have been due to undetected comorbid TDP-43.

The results of shape analysis may provide important insight into the functional outcomes of TDP-43 pathology in aging. Inward deformations of the laterobasal and superficial subdivisions of the amygdala were independently associated with TDP-43, as well as with AD and hippocampal sclerosis. The laterobasal subdivision is the main hub connecting the amygdala to the hippocampus, entorhinal cortex (Pikkarainen et al., 1999; Pitkänen et al., 2002), thalamus, and association sensory cortex (Price, 2003), and includes nuclei that are involved in emotional processing and storage of emotional memories (LeDoux and Schiller, 2009). The finding of laterobasal atrophy associated with TDP-43, AD, and hippocampal sclerosis is in agreement with memory deficits associated with all three neuropathologies (Wilson et al., 2013). The superficial subdivision of the amygdala has connections to the olfactory bulb and accessory olfactory bulb (Price, 2003). The finding of atrophy in the superficial subdivision associated with AD pathology may be related to the anosmia seen in AD (Doty, 2017). Although no studies have yet linked TDP-43 pathology in aging and hippocampal sclerosis to olfactory abnormalities, recently, TDP-43 pathology has been detected in the olfactory bulb of patients with AD (Josephs and Dickson, 2016), and TDP-43 has been linked to olfactory dysfunction in patients with amyotrophic lateral sclerosis (Takeda et al., 2014). The smaller spatial extent of the laterobasal and superficial deformations associated with TDP-43 compared to those associated with AD and hippocampal sclerosis, suggests that TDP-43 may be affecting fewer, or smaller portions of the, nuclei of these two subdivisions of the amygdala, implying more specialized cognitive and other clinical outcomes. In the centromedial subdivision of the amygdala inward deformation was mainly associated with TDP-43 pathology. The centromedial subdivision of the amygdala has connections to the brainstem, insula, hypothalamus, orbital and medial prefrontal cortex (Price, 2003), and has been linked to negative emotion, fear, anger, and aggressive behavior (Caparelli et al., 2017). The presence of TDP-43 pathology in patients with AD was recently linked to agitation/aggression (Sennik et al., 2017), supporting the findings of the present work. Aggressive behavior has also been linked to AD pathology (Sennik et al., 2017), and the lack of association of centromedial amygdala deformation with AD pathology in the present work suggests that aggression in AD may be a result of frontal lobe, instead of amygdala, abnormalities. This hypothesis is further supported by the fact that aggression typically develops in later stages of AD (Sennik et al., 2017), while amygdala is affected early on in AD (Poulin et al., 2011).

Author Manuscript Author Manuscript Author Manuscript Author Manuscript

Recent studies have shown that the majority of older adults with hippocampal sclerosis (not related to epilepsy or acute hypoxia) also suffer by TDP-43 (Nag et al., 2015; Zarow et al., 2012). In agreement with previous reports, 92% of participants with hippocampal sclerosis were TDP-43 positive in the present work. On the other hand, many older adults with TDP-43 do not have hippocampal sclerosis (83% of TDP-43 positive participants in this work) (Nag et al., 2015). It has been suggested that persons that are TDP-43 positive but don't have hippocampal sclerosis are in an early phase of the same disease as persons that are positive to both TDP-43 and hippocampal sclerosis (Hokkanen et al., 2018). However, the exact link between TDP-43 and hippocampal sclerosis has not yet been established, and therefore, in the present work, the two pathologies were considered separately. In contrast, participants with hippocampal sclerosis that were TDP-43 negative (a total of 2 persons) are not thought to be suffering by the same disease as those positive to only TDP-43 or both TDP-43 and hippocampal sclerosis. Those persons were excluded and the analysis was repeated, but the results remained essentially unchanged.

Amygdala volume explained an additional 8.1% of the variance of the rate of decline in global cognition, 5.3% in episodic memory, 8.7% in semantic memory, and 3.8% in perceptual speed, above and beyond what was explained by neuropathologies and demographics. The additional portion of the variance of the rate of cognitive decline explained by amygdala volume was substantial, and indicates that this metric captures additional decline-related structural differences across participants. These structural differences may be due to: a) known pathology types that were not measured fully, b) unknown pathology that was not assessed (Nelson et al., 2018), or c) environmental or experiential factors (Maguire et al., 2000).

The findings of the present work based on ex-vivo MRI are expected to translate well to the in-vivo case, based on previous work using the same methodology (Dawe et al., 2011; Kotrotsou et al., 2015, 2014). More specifically, it has been shown that, for the experimental approach used here, a linear relationship exists between structural brain information collected ex-vivo and in-vivo on the same individuals (Kotrotsou et al., 2014). Furthermore, there is good agreement in several volumetric and shape analysis findings between previously published studies that used the same ex-vivo MRI methodology and in-vivo work (Dawe et al., 2011; Kotrotsou et al., 2015).

One limitation of the current investigation is that, since imaging was conducted ex-vivo, the intracranial volume was not available. However, the height of the participants was used for normalization in the volumetric and shape analysis, which has previously been used as a surrogate for total intracranial volume. Also, laterality was not considered since only one hemisphere from each participant was studied, and left and right amygdalas were combined (after mirroring) in the analyses to maximize the degrees of freedom. In addition, only the score for TDP-43 pathology included measurements in the amygdala, among other regions, while the scores for the other pathologies were based on measurements in other predefined brain regions, following the established protocol of the parent studies (MAP, ROS) which has been presented in a number of publications. Measuring all pathologies in the amygdala is a goal of future studies. Another limitation is that, since the amygdala degenerates simultaneously with other brain regions that were not considered here, and given the fact

Author Manuscript Author Manuscript Author Manuscript Author Manuscript

that amygdala is mainly involved in behavior and emotion and has a lesser role in cognition, the additional portion of the variance of the rate of cognitive decline explained in this work may not be specific to the amygdala. Finally, the imaging voxels were not cubic. However, the voxel volume was $0.5mm^3$, which is smaller than that of most investigations of amygdala structure.

The present work demonstrated that TDP-43 pathology in aging not only has a significant independent negative association with the volume of the amygdala after correcting for the effects of other neuropathologies, but is also associated with a unique spatial pattern of inward deformation of the amygdala surface that is different than the patterns linked to AD pathology and hippocampal sclerosis. These findings may enhance future MR-based biomarkers. Finally, the volume of the amygdala was shown to capture additional structural contributions to the variance of the rate of cognitive decline, above and beyond what was captured by neuropathologies and demographics, suggesting that ex-vivo MRI may play an important role in enhancing our understanding of cognitive aging.

Acknowledgements

The authors would like to thank the participants and staff of the Rush Memory and Aging Project and the Religious Orders Study. The study was supported by NIH grants P30AG010161, UH2NS100599, R01AG042210, R01AG17917, R01AG34374, and the Illinois Department of Public Health (Alzheimer's Disease Research Fund).

Abbreviations:

TDP-43	Transactive response DNA-binding protein 43
AD	Alzheimer's disease

References

Amunts K, Kedo O, Kindler M, Pieperhoff P, Mohlberg H, Shah NJ, Habel U, Schneider F, Zilles K, 2005 Cytoarchitectonic mapping of the human amygdala, hippocampal region and entorhinal cortex: intersubject variability and probability maps. Anat. Embryol. (Berl). 210, 343–52. doi: 10.1007/s00429-005-0025-5 [PubMed: 16208455]

Arai T, Mackenzie IRA, Hasegawa M, Nonoka T, Niizato K, Tsuchiya K, Iritani S, Onaya M, Akiyama H, 2009 Phosphorylated TDP-43 in Alzheimer's disease and dementia with Lewy bodies. Acta Neuropathol. 117, 125–136. doi:10.1007/s00401-008-0480-1 [PubMed: 19139911]

Arnold SJ, Dugger BN, Beach TG, 2013 TDP-43 deposition in prospectively followed, cognitively normal elderly individuals: Correlation with argyrophilic grains but not other concomitant pathologies. Acta Neuropathol. 126, 51–57. doi:10.1007/s00401-013-1110-0 [PubMed: 23604587]

Arvanitakis Z, Leurgans SE, Barnes LL, Bennett DA, Schneider JA, 2011a Microinfarct pathology, dementia, and cognitive systems. Stroke 42, 722–7. doi:10.1161/STROKEAHA.110.595082 [PubMed: 21212395]

Arvanitakis Z, Leurgans SE, Wang Z, Wilson RS, Bennett DA, Schneider JA, 2011b Cerebral amyloid angiopathy pathology and cognitive domains in older persons. Ann. Neurol. 69, 320–7. doi:10.1002/ana.22112 [PubMed: 21387377]

Benjamini Y, Hochberg Y, 1995 Controlling the false discovery rate: a practical and powerful approach to multiple testing. J. R. Stat. Soc. B. doi:10.2307/2346101

Bennett DA, Buchman AS, Boyle PA, Barnes LL, Wilson RS, Schneider JA, 2018 Religious Orders Study and Rush Memory and Aging Project. J. Alzheimer's Dis. 64, S161–S189. doi:10.3233/JAD-179939 [PubMed: 29865057]

Author Manuscript Author Manuscript Author Manuscript Author Manuscript

Bennett DA, Schneider JA, Aggarwal NT, Arvanitakis Z, Shah RC, Kelly JF, Fox JH, Cochran EJ, Arends D, Treinkman AD, Wilson RS, 2006 Decision rules guiding the clinical diagnosis of Alzheimer's disease in two community-based cohort studies compared to standard practice in a clinic-based cohort study. Neuroepidemiology 27, 169–76. doi:10.1159/000096129 [PubMed: 17035694]

Bennett DA, Wilson RS, Schneider JA, Evans DA, Beckett LA, Aggarwal NT, Barnes LL, Fox JH, Bach J, 2002 Natural history of mild cognitive impairment in older persons. Neurology 59, 198–205. [PubMed: 12136057]

Boyle PA, Wilson RS, Aggarwal NT, Tang Y, Bennett DA, 2006 Mild cognitive impairment: risk of Alzheimer disease and rate of cognitive decline. Neurology 67, 441–5. doi:10.1212/01.wnl.0000228244.10416.20 [PubMed: 16894105]

Caparelli EC, Ross TJ, Gu H, Liang X, Stein EA, Yang Y, 2017 Graph theory reveals amygdala modules consistent with its anatomical subdivisions. Sci. Rep. 7, 14392. doi:10.1038/s41598-017-14613-4 [PubMed: 29089582]

Cavedo E, Boccardi M, Ganzola R, Canu E, Beltramello A, Caltagirone C, Thompson PM, Frisoni GB, 2011 Local amygdala structural differences with 3T MRI in patients with Alzheimer disease. Neurology 76, 727–33. doi:10.1212/WNL.0b013e31820d62d9 [PubMed: 21339500]

Davidson YS, Raby S, Foulds PG, Robinson A, Thompson JC, Sikkink S, Yusuf I, Amin H, Duplessis D, Troakes C, Al-Sarraj S, Sloan C, Esiri MM, Prasher VP, Allsop D, Neary D, Pickering-Brown SM, Snowden JS, Mann DMA, 2011 TDP-43 pathological changes in early onset familial and sporadic Alzheimer's disease, late onset Alzheimer's disease and Down's Syndrome: Association with age, hippocampal sclerosis and clinical phenotype. Acta Neuropathol. 122, 703–713. doi:10.1007/s00401-011-0879-y [PubMed: 21968532]

Dawe RJ, Bennett DA, Schneider JA, Arfanakis K, 2011 Neuropathologic correlates of hippocampal atrophy in the elderly: A clinical, pathologic, postmortem MRI study. PLoS One 6. doi:10.1371/journal.pone.0026286

Dawe RJ, Bennett DA, Schneider JA, Leurgans SE, Kotrotsou A, Boyle PA, Arfanakis K, 2014 Ex vivo T2 relaxation: associations with age-related neuropathology and cognition. Neurobiol. Aging 35, 1549–61. doi:10.1016/j.neurobiolaging.2014.01.144 [PubMed: 24582637]

Doty RL, 2017 Olfactory dysfunction in neurodegenerative diseases: is there a common pathological substrate? Lancet Neurol. 16, 478–488. doi:10.1016/S1474-4422(17)30123-0 [PubMed: 28504111]

Freeman SH, Spires-Jones T, Hyman BT, Growdon JH, Frosch MP, 2008 TAR-DNA binding protein 43 in Pick disease. J. Neuropathol. Exp. Neurol. 67, 62–7. doi:10.1097/nen.0b013e3181609361 [PubMed: 18091558]

Fujishiro H, Uchikado H, Arai T, Hasegawa M, Akiyama H, Yokota O, Tsuchiya K, Togo T, Iseki E, Hirayasu Y, 2009 Accumulation of phosphorylated TDP-43 in brains of patients with argyrophilic grain disease. Acta Neuropathol. 117, 151–158. doi:10.1007/s00401-008-0463-2 [PubMed: 19039597]

Geser F, Robinson JL, Malunda JA, Xie SX, Clark CM, Kwong LK, Moberg PJ, Moore EM, Van Deerlin VM, Lee VM-Y, Arnold SE, Trojanowski JQ, 2010 Pathological 43-kDa Transactivation Response DNA-Binding Protein in Older Adults With and Without Severe Mental Illness. Arch. Neurol. 67, 1238–1250. doi:10.1001/archneurol.2010.254 [PubMed: 20937952]

Geser F, Winton MJ, Kwong LK, Xu Y, Xie SX, Igaz LM, Garruto RM, Perl DP, Galasko D, Lee VMY, Trojanowski JQ, 2008 Pathological TDP-43 in parkinsonism-dementia complex and amyotrophic lateral sclerosis of Guam. Acta Neuropathol. 115, 133–145. doi:10.1007/s00401-007-0257-y [PubMed: 17713769]

Hokkanen SRK, Hunter S, Polvikoski TM, Keage HAD, Minett T, Matthews FE, Brayne C, 2018 Hippocampal sclerosis, hippocampal neuron loss patterns and TDP-43 in the aged population 28, 548–559. doi:10.1111/bpa.12556

James BD, Wilson RS, Boyle PA, Trojanowski JQ, Bennett DA, Schneider JA, 2016 TDP-43 stage, mixed pathologies, and clinical Alzheimer's-type dementia. Brain 139, 2983–2993. doi:10.1093/brain/aww224 [PubMed: 27694152]

Josephs KA, 2010 Dementia and the TAR DNA Binding Protein 43. Clin. Pharmacol. Ther. 88, 555–558. doi:10.1038/clpt.2010.112 [PubMed: 20739922]

Author Manuscript Author Manuscript Author Manuscript Author Manuscript

Josephs KA, Dickson DW, 2016 TDP-43 in the olfactory bulb in Alzheimer's disease. Neuropathol. Appl. Neurobiol. 42, 390–393. doi:10.1111/nan.12309 [PubMed: 26810591]

Josephs KA, Murray ME, Whitwell JL, Parisi JE, Petrucelli L, Jack CR, Petersen RC, Dickson DW, 2014a Staging TDP-43 pathology in Alzheimer's disease. Acta Neuropathol. 127, 441–50. doi: 10.1007/s00401-013-1211-9 [PubMed: 24240737]

Josephs KA, Whitwell JL, Weigand SD, Murray ME, Tosakulwong N, Liesinger AM, Petrucelli L, Senjem ML, Knopman DS, Boeve BF, Ivnik RJ, Smith GE, Jack CR, Parisi JE, Petersen RC, Dickson DW, 2014b TDP-43 is a key player in the clinical features associated with Alzheimer's disease. Acta Neuropathol. 127, 811–824. doi:10.1007/s00401-014-1269-z [PubMed: 24659241]

Koga S, Sanchez-Contreras M, Josephs KA, Uitti RJ, Graff-Radford N, van Gerpen JA, Cheshire WP, Wszolek ZK, Rademakers R, Dickson DW, 2016 Distribution and characteristics of transactive response DNA binding protein 43 kDa pathology in progressive supranuclear palsy. Mov. Disord. 32, 246–255. doi:10.1002/mds.26809 [PubMed: 28009087]

Kotrotsou A, Bennett DA, Schneider JA, Dawe RJ, Golak T, Leurgans SE, Yu L, Arfanakis K, 2014 Ex vivo MR volumetry of human brain hemispheres. Magn. Reson. Med. 71. doi:10.1002/mrm.24661 [PubMed: 25043333]

Kotrotsou A, Schneider JA, Bennett DA, Leurgans SE, Dawe RJ, Boyle PA, Golak T, Arfanakis K, 2015 Neuropathologic correlates of regional brain volumes in a community cohort of older adults. Neurobiol. Aging 36, 2798–2805. doi:10.1016/j.neurobiolaging.2015.06.025 [PubMed: 26195068]

Kromer Vogt LJ, Hyman BT, Van Hoesen GW, Damasio AR, 1990 Pathological alterations in the amygdala in Alzheimer's disease. Neuroscience 37, 377–85. [PubMed: 2133349]

LeDoux JE, Schiller D, 2009 What animal fear models have taught us about human amygdala function?, in: Whalen PJ, Phelps EA (Eds.), The Human Amygdala. Guilford Press, New York, NY, pp. 43–60.

Lippa CF, Rosso AL, Stutzbach LD, Neumann M, Lee VM, Trojanowski JQ, 2010 NIH Public Access. Response 66, 1483–1488. doi:10.1001/archneurol.2009.277.Transactive

Maguire E. a, Gadian DG, Johnsrude IS, Good CD, Ashburner J, Frackowiak RS, Frith CD, 2000 Navigation-related structural change in the hippocampi of taxi drivers. Proc. Natl. Acad. Sci. U. S. A. 97, 4398–403. doi:10.1073/pnas.070039597 [PubMed: 10716738]

Mcaleese KE, Walker L, Erskine D, Thomas AJ, Mckeith IG, Attems J, 2016 TDP-43 pathology in Alzheimer's disease, dementia with Lewy bodies and ageing. Brain Pathol. 1–8. doi:10.1111/bpa.12424

McKeith IG, Galasko D, Kosaka K, Perry EK, Dickson DW, Hansen LA, Salmon DP, Lowe J, Mirra SS, Byrne EJ, Lennox G, Quinn NP, Edwardson JA, Ince PG, Bergeron C, Burns A, Miller BL, Lovestone S, Collerton D, Jansen ENH, Ballard C, de Vos RAI, Wilcock GK, Jellinger KA, Perry RH, 1996 Consensus guidelines for the clinical and pathologic diagnosis of dementia with Lewy bodies (DLB). Neurology 47, 1113 LP-1124. [PubMed: 8909416]

McKhann G, Drachman D, Folstein M, Katzman R, Price D, Stadlan EM, 1984 Clinical diagnosis of Alzheimer's disease: report of the NINCDS-ADRDA Work Group under the auspices of Department of Health and Human Services Task Force on Alzheimer's Disease. Neurology 34, 939–44. [PubMed: 6610841]

Miller MI, Younes L, Ratnanather JT, Brown T, Trinh H, Lee DS, Tward D, Mahon PB, Mori S, Albert M, 2015 Amygdalar atrophy in symptomatic Alzheimer's disease based on diffeomorphometry: The BIOCARD cohort. Neurobiol. Aging 36, S3–S10. doi:10.1016/j.neurobiolaging.2014.06.032 [PubMed: 25444602]

Nag S, Yu L, Boyle PA, Leurgans SE, Bennett DA, Schneider JA, 2018 TDP-43 pathology in anterior temporal pole cortex in aging and Alzheimer ' s disease 1–11.

Nag S, Yu L, Capuano AW, Wilson RS, Leurgans SE, Bennett DA, Schneider JA, 2015 Hippocampal sclerosis and TDP-43 pathology in aging and Alzheimer disease. Ann. Neurol. 77, 942–52. doi: 10.1002/ana.24388 [PubMed: 25707479]

Nelson PT, Abner EL, Patel E, Anderson S, Wilcock DM, Kryscio RJ, Van Eldik LJ, Jicha GA, Gal Z, Nelson RS, Nelson BG, Gal J, Azam MT, Fardo DW, Cykowski MD, 2018 The Amygdala as a Locus of Pathologic Misfolding in Neurodegenerative Diseases. J. Neuropathol. Exp. Neurol. 77, 2–20. doi:10.1093/jnen/nlx099 [PubMed: 29186501]

Author Manuscript Author Manuscript Author Manuscript Author Manuscript

Nelson PT, Abner EL, Schmitt FA, Kryscio RJ, Jicha GA, Smith CD, Davis DG, Poduska JW, Patel E, Mendiondo MS, Markesbery WR, 2010 Modeling the Association between 43 Different Clinical and Pathological Variables and the Severity of Cognitive Impairment in a Large Autopsy Cohort of Elderly Persons. Brain Pathol. 20, 66–79. doi:10.1111/j.1750-3639.2008.00244.x [PubMed: 19021630]

Neumann M, Sampathu DM, Kwong LK, Truax AC, Micsenyi MC, Chou TT, Bruce J, Schuck T, Grossman M, Clark CM, McCluskey LF, Miller BL, Masliah E, Mackenzie IR, Feldman H, Feiden W, Kretzschmar HA, Trojanowski JQ, Lee VM-Y, 2006 Ubiquitinated TDP-43 in Frontotemporal Lobar Degeneration and Amyotrophic Lateral Sclerosis. Science (80-.). 314, 130–133. doi:10.1126/science.1134108

Olivé M, Janué A, Moreno D, Gámez J, Torrejón-Escribano B, Ferrer I, 2009 TAR DNA-Binding protein 43 accumulation in protein aggregate myopathies. J. Neuropathol. Exp. Neurol. 68, 262–73. doi:10.1097/NEN.0b013e3181996d8f [PubMed: 19225410]

Pikkarainen M, Rönkkö S, Savander V, Insausti R, Pitkänen A, 1999 Projections from the lateral, basal, and accessory basal nuclei of the amygdala to the hippocampal formation in rat. J. Comp. Neurol. 403, 229–60. [PubMed: 9886046]

Pitkänen A, Kelly JL, Amaral DG, 2002 Projections from the lateral, basal, and accessory basal nuclei of the amygdala to the entorhinal cortex in the macaque monkey. Hippocampus 12, 186–205. doi:10.1002/hipo.1099 [PubMed: 12000118]

Poulin SP, Dautoff R, Morris JC, Barrett LF, Dickerson BC, Alzheimer's Disease Neuroimaging Initiative, 2011 Amygdala atrophy is prominent in early Alzheimer's disease and relates to symptom severity. Psychiatry Res. 194, 7–13. doi:10.1016/j.pscychresns.2011.06.014 [PubMed: 21920712]

Price JL, 2003 Comparative aspects of amygdala connectivity. Ann. N. Y. Acad. Sci. 985, 50–8. [PubMed: 12724147]

Qiu A, Fennema-Notestine C, Dale AM, Miller MI, 2009 Regional shape abnormalities in mild cognitive impairment and Alzheimer's disease. Neuroimage 45, 656–661. doi:10.1016/j.neuroimage.2009.01.013 [PubMed: 19280688]

Schneider JA, Arvanitakis Z, Leurgans SE, Bennett DA, 2009 The neuropathology of probable Alzheimer disease and mild cognitive impairment. Ann. Neurol. 66, 200–8. doi:10.1002/ana.21706 [PubMed: 19743450]

Schneider JA, Arvanitakis Z, Yu L, Boyle PA, Leurgans SE, Bennett DA, 2012 Cognitive impairment, decline and fluctuations in older community-dwelling subjects with Lewy bodies. Brain 135, 3005–14. doi:10.1093/brain/aws234 [PubMed: 23065790]

Schneider JA, Boyle PA, Arvanitakis Z, Bienias JL, Bennett DA, 2007 Subcortical infarcts, Alzheimer's disease pathology, and memory function in older persons. Ann. Neurol. 62, 59–66. doi:10.1002/ana.21142 [PubMed: 17503514]

Schwab C, Arai T, Hasegawa M, Akiyama H, Yu S, McGeer PL, 2009 TDP-43 pathology in familial British dementia. Acta Neuropathol. 118, 303–311. doi:10.1007/s00401-009-0514-3 [PubMed: 19283396]

Schwab C, Arai T, Hasegawa M, Yu S, Mcgeer PL, 2008 Colocalization of Transactivation-Responsive DNA-Binding Protein 43 and Huntingtin in Inclusions of Huntington Disease. J Neuropathol Exp Neurol 67, 1159–1165. doi:10.1097/NEN.0b013e31818e8951 [PubMed: 19018245]

Sennik S, Schweizer TA, Fischer CE, Munoz DG, 2017 Risk Factors and Pathological Substrates Associated with Agitation/Aggression in Alzheimer's Disease: A Preliminary Study using NACC Data. J. Alzheimers. Dis. 55, 1519–1528. doi:10.3233/JAD-160780 [PubMed: 27911311]

Smith SM, Jenkinson M, Woolrich MW, Beckmann CF, Behrens TEJ, Johansen-Berg H, Bannister PR, De Luca M, Drobnjak I, Flitney DE, Niazy RK, Saunders J, Vickers J, Zhang Y, De Stefano N, Brady JM, Matthews PM, 2004 Advances in functional and structural MR image analysis and implementation as FSL. Neuroimage 23 Suppl 1, S208–19. doi:10.1016/j.neuroimage.2004.07.051 [PubMed: 15501092]

Styner M, Oguz I, Xu S, Brechbühler C, Pantazis D, Levitt JJ, Shenton ME, Gerig G, 2006 Framework for the Statistical Shape Analysis of Brain Structures using SPHARM-PDM. Insight J. m, 242–250.

Author Manuscript Author Manuscript Author Manuscript Author Manuscript

Styner MA, Rajamani KT, Nolte L-P, Zsemlye G, Székely G, Taylor CJ, Davies RH, 2003 Evaluation of 3D correspondence methods for model building. Inf. Process. Med. Imaging 2732, 63–75.

Takeda T, Uchihara T, Kawamura S, Ohashi T, 2014 Olfactory dysfunction related to TDP-43 pathology in amyotrophic lateral sclerosis. Clin. Neuropathol. 33, 65–67. doi:10.5414/NP300661 [PubMed: 24131749]

Tang X, Holland D, Dale AM, Younes L, Miller MI, 2015 The diffeomorphometry of regional shape change rates and its relevance to cognitive deterioration in mild cognitive impairment and Alzheimer's disease. Hum. Brain Mapp. 36, 2093–2117. doi:10.1002/hbm.22758 [PubMed: 25644981]

Tang X, Holland D, Dale AM, Younes L, Miller MI, 2014 Shape abnormalities of subcortical and ventricular structures in mild cognitive impairment and Alzheimer's disease: Detecting, quantifying, and predicting. Hum. Brain Mapp. 35, 3701–3725. doi:10.1002/hbm.22431 [PubMed: 24443091]

Tang X, Varma VR, Miller MI, Carlson MC, 2017 Education is associated with sub-regions of the hippocampus and the amygdala vulnerable to neuropathologies of Alzheimer's disease. Brain Struct. Funct. 222, 1469–1479. doi:10.1007/s00429-016-1287-9 [PubMed: 27535407]

Tremblay C, St-Amour I, Schneider J, Bennett DA, Calon F, 2011 Accumulation of transactive response DNA binding protein 43 in mild cognitive impairment and Alzheimer disease **. J. Neuropathol. Exp. Neurol. 70, 788–98. doi:10.1097/NEN.0b013e31822c62cf [PubMed: 21865887]

Uchino A, Takao M, Hatsuta H, Sumikura H, Nakano Y, Nogami A, Saito Y, Arai T, Nishiyama K, Murayama S, 2015 Incidence and extent of TDP-43 accumulation in aging human brain. Acta Neuropathol. Commun. 3, 35. doi:10.1186/s40478-015-0215-1 [PubMed: 26091809]

Uryu K, Nakashima-yasuda H, Forman MS, Kretzschmar HA, Lee VM, Trojanowski JQ, 2013 NIH Public Access 67, 555–564. doi:10.1097/NEN.0b013e31817713b5.Concomitant

Van Petten C, 2004 Relationship between hippocampal volume and memory ability in healthy individuals across the lifespan: Review and meta-analysis. Neuropsychologia 42, 1394–1413. doi:10.1016/j.neuropsychologia.2004.04.006 [PubMed: 15193947]

Wider C, Dickson DW, Stoessl AJ, Tsuboi Y, Chapon F, Gutmann L, Lechevalier B, Calne DB, Personett DA, Hulihan M, Kachergus J, Rademakers R, Baker MC, Grantier LL, Sujith OK, Brown L, Calne S, Farrer MJ, Wszolek ZK, 2009 Pallidonigral TDP-43 pathology in Perry syndrome. Park. Relat. Disord. 15, 281–286. doi:10.1016/j.parkreldis.2008.07.005

Wilson R, Barnes L, Bennett D, 2003 Assessment of lifetime participation in cognitively stimulating activities. J. Clin. Exp. Neuropsychol. 25, 634–42. doi:10.1076/jcen.25.5.634.14572 [PubMed: 12815501]

Wilson RS, Yu L, Trojanowski JQ, Chen E-Y, Boyle PA, Bennett DA, Schneider JA, 2013 TDP-43 Pathology, Cognitive Decline, and Dementia in Old Age. JAMA Neurol. 70, 1418. doi:10.1001/jamaneurol.2013.3961 [PubMed: 24080705]

Yokota O, Davidson Y, Arai T, Hasegawa M, Akiyama H, Ishizu H, Terada S, Sikkink S, Pickering-Brown S, Mann DMA, 2010 Effect of topographical distribution of ??-synuclein pathology on TDP-43 accumulation in Lewy body disease. Acta Neuropathol. 120, 789–801. doi:10.1007/s00401-010-0731-9 [PubMed: 20669025]

Yu L, De Jager PL, Yang J, Trojanowski JQ, Bennett DA, Schneider JA, 2015 The TMEM106B locus and TDP-43 pathology in older persons without FTLD. Neurology 84, 927–34. doi:10.1212/WNL.0000000000001313 [PubMed: 25653292]

Zarow C, Weiner MW, Ellis WG, Chui HC, 2012 Prevalence, laterality, and comorbidity of hippocampal sclerosis in an autopsy sample. Brain Behav. 2, 435–442. doi:10.1002/brb3.66 [PubMed: 22950047]

Author Manuscript Author Manuscript Author Manuscript Author Manuscript

Highlights

- TDP-43 is linked to lower amygdala volume, independent of other pathologies
- TDP-43 is associated with a unique spatial pattern of amygdala deformation
- Amygdala volume captures variance in cognitive decline not explained by pathologies

Author Manuscript Author Manuscript Author Manuscript Author Manuscript

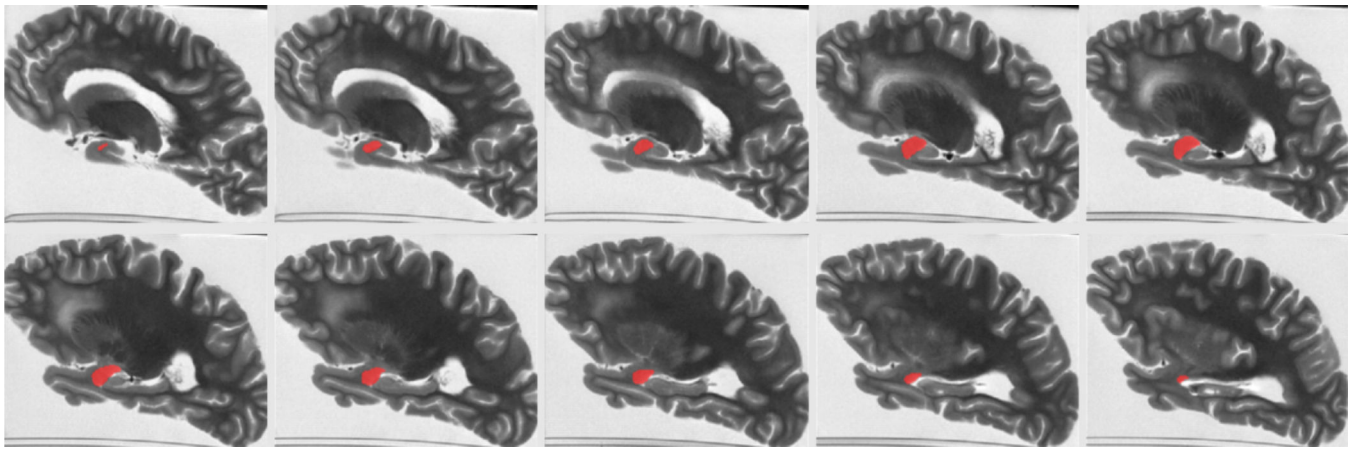

Figure 1.
An example of amygdala segmentation for a cerebral hemisphere of one of the participants.

Author Manuscript Author Manuscript Author Manuscript Author Manuscript

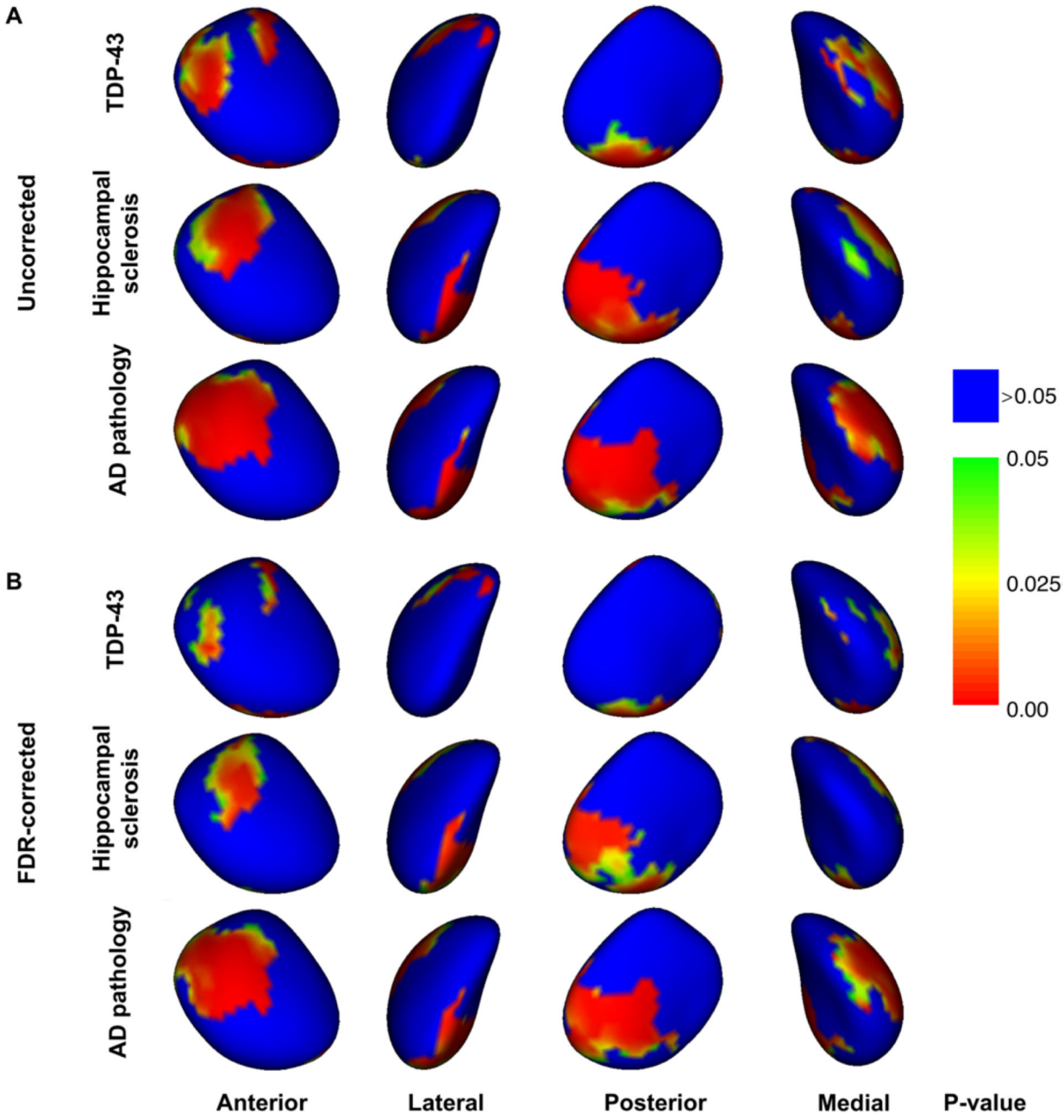

Figure 2.

(A) Un-corrected and (B) FDR-corrected significance maps demonstrating statistically significant inward deformation of the surface of the amygdala associated with TDP-43 pathology in aging, hippocampal sclerosis, and AD pathology (controlling for other neuropathologies, demographics and covariates). Red, yellow, and green colors indicate significant effects ($p<0.05$).

Author Manuscript Author Manuscript Author Manuscript Author Manuscript

Table 1.

Demographic and clinical characteristics of the participants

Characteristics	Total
N	198
Age at death, years (SD)	90 (6)
Male, n (%)	57 (29%)
Education, years (SD)	16 (4)
Years of clinical follow-up, mean (SD)	8 (5)
Median time between last evaluation and death, years (interquartile range)	0.78 (0.4–1.2)
Clinical diagnosis proximate to death, n (%)	
- No cognitive impairment	55 (28%)
- Mild cognitive impairment	43 (22%)
- Dementia	100 (50%)
Global cognition score[a], mean (SD)	−1.1 (1.2)
Episodic memory score[a], mean (SD)	−1.0 (1.4)
Semantic memory score[a], mean (SD)	−1.4 (1.6)
Working memory score[a], mean (SD)	−0.9 (1.1)
Perceptual speed score[a], mean (SD)	−1.3 (1.2)
Visuospatial ability score[a], mean (SD)	−0.7 (1.2)
Mini-mental State Examination[a] (MMSE), mean (SD)	19.5 (9.6)
Mini-mental State Examination[a] (MMSE), median	23.4
Right hemisphere, n (%)	93 (47%)
Postmortem interval to fixation, hours (SD)	8.6 (6.5)
Postmortem interval to imaging, days (SD)	49.6 (24.0)
MRI scanner, n (%)	
- General Electric, 3 Tesla, n (%) **Participants with TDP-43, n (%)**	48 (24%) 22 (46%)
- Philips, 3 Tesla, n (%) **Participants with TDP-43, n (%)**	85 (43%) 27 (32%)
- Siemens, 3 Tesla, n (%) **Participants with TDP-43, n (%)**	65 (33%) 22 (34%)

[a]Proximate to death

Author Manuscript

Author Manuscript

Author Manuscript

Author Manuscript

Table 2.

Neuropathologic characteristics of the participants

Characteristics	Total
NIA Reagan (Likelihood of AD), n (%)	
-High or Intermediate Likelihood	137 (69%)
-Low Likelihood or No AD	61 (31%)
Composite score of global AD pathology, mean (SD)	0.8 (0.6)
Lewy bodies, n (%)	43 (22%)
Hippocampal sclerosis, n (%)	24 (12%)
Gross infarcts, n (%)	93 (47%)
Microscopic infarcts, n (%)	73 (37%)
Atherosclerosis, n (%)	
-Severe	23 (12%)
-Moderate	53 (27%)
-Mild	87 (44%)
-None	35 (18%)
Arteriosclerosis, n (%)	
-Severe	20 (10%)
-Moderate	34 (17%)
-Mild	93 (47%)
-None	51 (26%)
Cerebral amyoid angiopathy, n (%)	
-Severe	19 (10%)
-Moderate	51 (26%)
-Mild	92 (47%)
-None	36 (18%)
TDP-43, n (%)	
-inclusions in amygdala, entorhinal cortex or hippocampus CA1, and neocortex	28 (14%)
-inclusions in amygdala and entorhinal cortex or hippocampus CA1	58 (30%)
-inclusions in amygdala only	41 (21%)
-no inclusions	71 (36%)

Author Manuscript

Author Manuscript

Author Manuscript

Author Manuscript

Table 3.

Association of amygdala volume with rate of change in different cognitive domains, based on mixed-effects models controlling for neuropathologies and demographics[a].

	Estimate (p-value)	Percentage of variance of the rate of change explained by amygdala volume
Global cognition	**$1.8 \cdot 10^{-4}$ (0.009)**	8.1%
Episodic memory	**$1.7 \cdot 10^{-4}$ (0.027)**	5.3%
Semantic memory	**$2.4 \cdot 10^{-4}$ (0.0012)**	8.7%
Working memory	$-6 \cdot 10^{-6}$ (0.93)	-
Perceptual speed	**$1.8 \cdot 10^{-4}$ (0.029)**	3.8%
Visuospatial abilities	$8 \cdot 10^{-5}$ (0.26)	-

[a] The middle column shows the model estimates and corresponding p-values for the interaction of amygdala volume with time since baseline, in mixed-effects models where the longitudinal dependent variable was the cognitive score, and the independent variables were all the neuropathologies, demographics, amygdala volume, as well as the interaction of each one of these variables with time since baseline. The rightmost column shows the contribution of amygdala volume to the variance of the rate of change in different cognitive domains, above and beyond the contributions of neuropathologies and demographics (based on two mixedeffects models, with and without terms for amygdala volume and its interaction with time since baseline).